Infrared–x-ray pump-probe spectroscopy of the NO molecule

F. F. Guimarães,[1,2] V. Kimberg,[1] V. C. Felicíssimo,[1,2] F. Gel'mukhanov,[1] A. Cesar,[2] and H. Ågren[1]
[1]*Theoretical Chemistry, Roslagstullsbacken 15, Royal Institute of Technology, S-106 91 Stockholm, Sweden*
[2]*Departamento de Química, Universidade Federal de Minas Gerais, Avenida Antonio Carlos, 6627, CEP-31270-901, Belo Horizonte, Minas Gerais, Brazil*

(Received 24 November 2004; published 22 July 2005)

Two color infrared–x-ray pump-probe spectroscopy of the NO molecule is studied theoretically and numerically in order to obtain a deeper insight of the underlying physics and of the potential of this suggested technology. From the theoretical investigation a number of conclusions could be drawn: It is found that the phase of the infrared field strongly influences the trajectory of the nuclear wave packet, and hence, the x-ray spectrum. The trajectory experiences fast oscillations with the vibrational frequency with a modulation due to the anharmonicity of the potential. The dependences of the x-ray spectra on the delay time, the duration, and the shape of the pulses are studied in detail. It is shown that the x-ray spectrum keep memory about the infrared phase after the pump field left the system. This memory effect is sensitive to the time of switching-off the pump field and the Rabi frequency. The phase effect takes maximum value when the duration of the x-ray pulse is one-fourth of the infrared field period, and can be enhanced by a proper control of the duration and intensity of the pump pulse. The manifestation of the phase is different for oriented and disordered molecules and depends strongly on the intensity of the pump radiation.

DOI: 10.1103/PhysRevA.72.012714 PACS number(s): 33.80.Eh, 33.70.Ca

I. INTRODUCTION

Coherent superposition of states is a key concept in contemporary quantum physics. Various superpositions of molecular states or wave packets can be created in strong fields generated by infrared or optical lasers. One can expect that coherent properties of the light are transferred to the molecule, which means that the evolution of the wave packet must be sensitive to the phase of the pump radiation. This leads to the idea to probe the phase sensitive dynamics of the molecular wave packet by means of x-ray radiation. According to our knowledge the influence of the phase of the pump radiation on the wave packet trajectory and, hence, on x-ray probe signals has not been studied for a real system yet: In our companion paper we presented infrared–x-ray pump probe theory and applied this theory to study the proton transfer in the water dimer which constitutes an important prototype system containing a hydrogen bond [1]. The viability to perform core excitation in regions of the potential energy surface that are unavailable by standard x-ray absorption was there demonstrated [1], something that indicates the power of this kind of new experimental tool. In the present paper we address infrared (ir)–x-ray pump-probe spectroscopy of the NO molecule, as this simple one-dimensional system allows great numerical detail with strict solutions of the quantum equations and scrutiny of the underlying physics. This in turn allows one to pinpoint the optimal experimental conditions for ir–x-ray pump-probe spectroscopy and for measurements.

We point out the striking applications of time-resolved and phase sensitive ir–x-ray pump-probe experiments with a few-cycle 750-nm laser field and with a duration of the x-ray pulse of the order of femtoseconds [2]. Studies of phase sensitive dynamics of the molecular wave packet (WP) require quite short x-ray pulses, with a time lapse of 1–100 fs. As reviewed in [1] several kinds of such sources are available already today [3–6], in fact, ultrashort x-ray pulses as short as $\approx$250 as [2] have recently been reported. This indicates that x-ray pump-probe spectroscopy is able to explore the nuclear dynamics even by the use of current light sources.

The main aim of our paper is to investigate time and phase resolved x-ray absorption of nitrogen monoxide driven by a strong ir pulse. The pump radiation affects the x-ray absorption in two qualitatively different ways. The first one arises from an incoherent population of higher vibrational levels ("heating" effect) which takes place when the pump radiation is incoherent. Our simulations show very different x-ray spectra of the NO molecule in different initial vibrational states. A coherent pump pulse with permanent phase changes the scenario drastically as a coherent superposition of vibrational states then is created. This second way makes the dynamics of the nuclear wave packet phase sensitive. Due to the phase dependence of the trajectory of the wave packet, the x-ray spectrum becomes different for different phases and delay times. Because of the long lifetime of the vibrational levels the WP keeps the memory about the ir phase, which results in a memory effect in x-ray absorption. We would like to note that the phase effect which we study has nothing to do with the role of the phase in few-cycle experiments [7–9].

The paper is organized as follows. We start in Sec. II describing the physical picture of phase dependence of x-ray absorption. The wave packet formalism used in the simulations is described in Sec. III. The details of computations are elucidated in Sec. IV. We analyze the results of calculations of x-ray absorption of NO driven by a strong ir field in Sec. V. The experimental conditions for observation of the discussed phase effect are analyzed in Sec. VI. Our findings are summarized in Sec. VII.

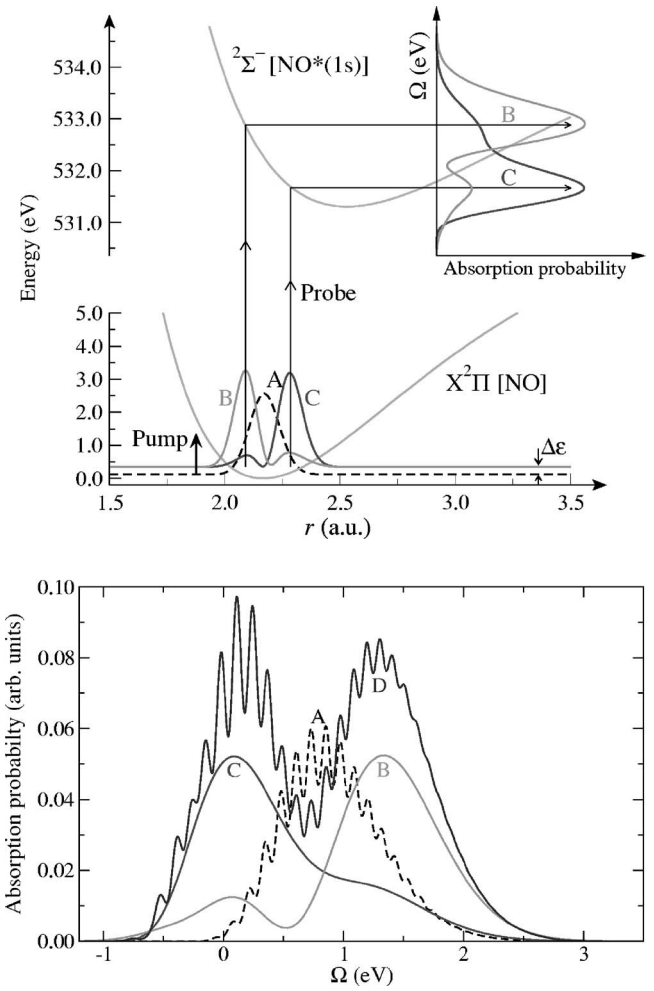

FIG. 1. Main spectral features of the O 1*s* x-ray absorption spectra ($^2\Pi \rightarrow {}^2\Sigma^-$) of the NO molecule in the strong ir field. $\varphi_L = 0$. $\omega_L = \omega_{10} = 0.241$ eV. $\mathbf{e}_L \| \mathbf{d}$. $\Delta\epsilon = \epsilon(t) - \epsilon_0$ [see Eq. (23)]. $\tau_L = 100$ fs. The wave packets and corresponding x-ray spectra are marked by labels A, B, and C. A: $I_L = 0$, $\tau_X = 15$ fs. B: $I_L = 2.3 \times 10^{12}$ W/cm^2, $\tau_X = 3$ fs, $\Delta t = 1035$ fs. C: $I_L = 2.3 \times 10^{12}$ W/cm^2, $\tau_X = 3$ fs, $\Delta t = 1025$ fs. D: $I_L = 2.3 \times 10^{12}$ W/cm^2, $\tau_X = 15$ fs, $\Delta t > 2(\tau_L + \tau_X)$.

II. PHYSICAL PICTURE OF THE PHASE SENSITIVITY OF X-RAY ABSORPTION SPECTRUM

To give insight into the physics of the studied effect it is instructive to start from a simplified picture. The phase effect [10] can be explained in two qualitatively different ways. We present both interpretations because they shed light on different aspects of the phase problem.

A. Interference of one- and many-photon absorption channels

We consider molecules which interact with the ir pump field (L) and high-frequency probe x-ray radiation field (X) (see Fig. 1):

$$\boldsymbol{\mathcal{E}}_\alpha(t) = \mathbf{E}_\alpha(t)\cos(\omega_\alpha t - \mathbf{k}_\alpha \cdot \mathbf{R} + \varphi_\alpha), \quad \alpha = L, X. \tag{1}$$

We use atomic units everywhere except in Sec. IV. The pump and probe fields, $\mathbf{E}_\alpha(t) = \mathbf{e}_\alpha E_\alpha(t)$, are characterized by the polarizations ($\mathbf{e}_\alpha$) and wave vectors ($\mathbf{k}_\alpha$), envelopes, $E_\alpha(t)$, frequencies, ω_α, and phases, $\varphi_\alpha = \varphi_\alpha(t)$, which in general are all time-dependent. The key idea behind x-ray pump-probe spectroscopy is straightforward. The strong ir field mixes coherently the vibrational levels in the ground electronic state. Because of this, the nuclear wave packet starts to move in the potential well. The proper choice of delay time for the x-ray pulse allows one to obtain snapshots of x-ray spectra at different site positions of the nuclear wave packet (see Fig. 1). As one can see from Fig. 1 such a technique allows one to map the shape of the excited state potential. We show that the x-ray spectra are very sensitive to the phase of ir field.

The interaction between the probe x-ray radiation and the molecule is influenced by the strong ir field which changes the populations of the vibrational levels (ν) of the ground electronic state. We ignore the ir mixing of vibrational levels in the final core-excited electronic state which is small due to the large lifetime broadening. Different channels of the x-ray absorption are possible, for example, direct one-photon absorption or $\nu+1$ absorption channel

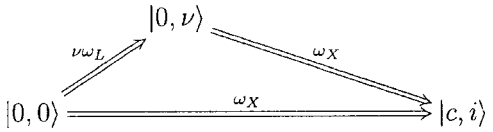

where $|j,\nu\rangle$ is the electron-vibrational state. The second channel corresponds to x-ray absorption from the vibrational level $|\nu\rangle$ of the ground electronic state excited due to absorption of ν ir photons: $|0\rangle \rightarrow |1\rangle \rightarrow |2\rangle \rightarrow \cdots |\nu\rangle$. The photoabsorption amplitude is the sum of one- and $(\nu+1)$-photon contributions, which can approximately be written as

$$\frac{(\mathbf{D}_{c0} \cdot \mathbf{E}_X)}{\omega_X - \omega_{ci,00} - i\Gamma} + \sum_{\nu=1}^{\infty} (\mathbf{d}_{10} \cdot \mathbf{E}_L) \cdots (\mathbf{d}_{\nu,\nu-1} \cdot \mathbf{E}_L) \times \left(\frac{e^{-i(\omega_L t + \varphi_L + \mathbf{k}_L \cdot \mathbf{R})}}{\Omega_L - i\Gamma_0} \right)^\nu \frac{(\mathbf{D}_{c0} \cdot \mathbf{E}_X)}{\omega_X - \omega_{ci,0\nu} - i\Gamma}. \tag{2}$$

Here $\Omega_L = \omega_L - \omega_{10}$ is the detuning of the ir field relative to the frequency of the resonance transition between first and lowest vibrational levels; Γ and Γ_0 are lifetime broadenings of the core excited state and vibrational levels of the ground state, respectively; $\omega_{ci,0\nu}$ is the resonant energy of the electron-vibrational transition $|0,\nu\rangle \rightarrow |c,i\rangle$; $\mathbf{d}_{\nu,\nu-1}$ is the transition dipole moment between adjusted vibrational levels, while $\mathbf{D}_{c0}$ is the dipole moment of the electronic transition between ground and core-excited electronic states. The expression for the absorption amplitude (2) represents a rather rough approximation. However, the simplicity of this expression makes it easy to understand the role of the phase of the x-ray absorption.

The x-ray absorption probability, which is the square of the amplitude (2), contains the interference term

$$P_{\text{int}}^{(\nu)}(t) \sim \left[\frac{e^{-i(\omega_L t + \varphi_L + \mathbf{k}_L \cdot \mathbf{R})}}{\Omega_L - i\Gamma_0} (\mathbf{d}_{10} \cdot \mathbf{E}_L) \right]^\nu |\mathbf{D}_{c0} \cdot \mathbf{e}_X|^2 E_X^* E_X \propto E_X(t) e^{-i\nu(\omega_L t + \varphi_L)}, \quad \nu = 1, 2, \ldots . \tag{3}$$

We assume in this estimate that the transition matrix ele-

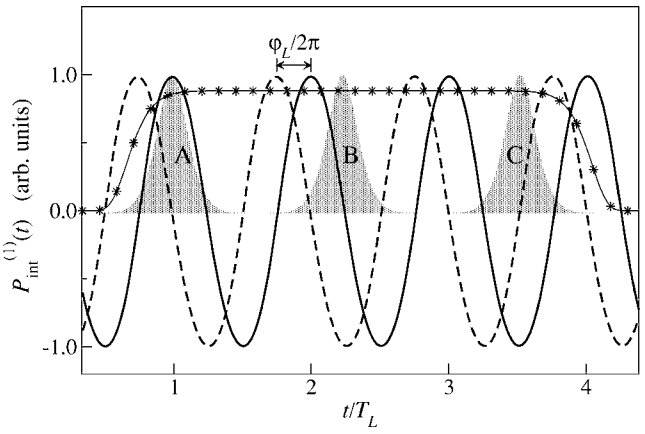

FIG. 2. Qualitative illustration of the dependence of the x-ray absorption probability on the ir phase φ_L and on the delay time Δt. The ir field for different phases is depicted by solid and broken lines. The labels A, B, and C mark short x-ray pulses ($\tau_X < T_L$) for different delay times. The curve marked by stars shows long x-ray pulse ($\tau_X \gg T_L$). $T_L = 2\pi/\omega_L$ is the period of oscillations of the ir field.

ments of the ir transitions, $\nu \rightarrow \nu+1$, are collinear; which is the case for diatomic molecules. Equation (3) shows directly the strong sensitivity of the x-ray absorption on the phase of the pump field, φ_L. Figure 2 shows the interference (3) of one- and two-photon channels ($\nu=1$) which results in that the signal beats with the ir frequency, ω_L. Such beats can be directly observed if the time resolution of the x-ray detector is better than the period of the oscillations of the ir field, $T_L = 2\pi/\omega_L$. According to our knowledge the current x-ray instrumentation allows one to measure only the signal integrated over time. In this case the phase sensitive interference term is quenched when the duration of the x-ray pulse, τ_X, is much longer than T_L (Fig. 2). The situation changes drastically for a short x-ray pulse, $\tau_X \sim T_L$, as such a pulse may select positive or negative parts of the oscillating ir field (Fig. 2). As one can see from Fig. 2, the sign and magnitude of the area of the ir field selected by a short x-ray pulse,

$$S(\varphi_L) = \int E_X(t)\cos(\omega_L t + \varphi_L)dt \neq 0,$$

are very sensitive to the phase of the ir field as well as to the delay time of the x-ray pulse relative to the pump pulse. One can expect that the x-ray spectrum of the molecule in the strong ir field also is sensitive to the phase of the ir field. More precisely, it is sensitive to the peak position of the x-ray pulse relative to the "comb" of the ir field. This means that the phase of the ir field and the delay time play quite similar roles, namely, one can change the peak position of the probe pulse relative to the ir comb with help of the ir phase or delay time (see Fig. 2). Let us explore this effect in more detail making use of a strict formalism.

B. Role of phase of ir field on the wave packet dynamics

The pump ir pulse $E_L(t)$ induces transitions between vibrational levels of the ground electronic state (or dissociates) and creates the nuclear WP

$$|\phi(t)\rangle = \sum_\nu a_\nu(t)|\nu\rangle e^{-i\epsilon_\nu t},$$

$$|\phi(0)\rangle = |0\rangle, \quad \langle\phi(t)|\phi(t)\rangle = 1. \tag{4}$$

Here ϵ_ν and $|\nu\rangle$ are the vibrational energy and eigenvector of the ground electronic state. The nuclear wave packet of the ground state (4) obeys the Schrödinger equation

$$i\frac{\partial}{\partial t}\phi(t) = H(t)\phi(t),$$

$$H(t) = H_0 - [\mathbf{d}\cdot\mathbf{E}_L(t)]\cos(\omega_L t + \varphi_L), \tag{5}$$

with H_0 as the nuclear Hamiltonian of the ground electronic state. The broadening of the vibrational levels of the ground state, Γ_0, is ignored here. This approximation is justified for diatomic molecules in gas phase which have very large vibrational state lifetimes ($\lesssim 1$ ms), much longer than the delay time and duration of x-ray pulse considered in this paper. Let us note that the spatial phases $\mathbf{k}_L\cdot\mathbf{R}$ and $\mathbf{k}_X\cdot\mathbf{R}$ are ignored in the remaining part of the paper. The role of these phases can be important and this approximation was already discussed in Ref. [10]. For instance, these phases can be neglected for perpendicular intersection of x-ray and ir pulses.

We solve the Schrödinger equation (5) using the rotating wave approximation, assuming the pump field to be weak and $\omega_L = \omega_{10}$:

$$a_1(t) = ie^{-i\varphi_L}\int_{-\infty}^{t} dt_1[\mathbf{d}_{10}\cdot\mathbf{E}_L(t_1)] = e^{-i\varphi_L}c_1(t), \quad a_0(t) \approx 1. \tag{6}$$

One can see that contrary to $a_0(t) \approx 1$ the amplitude of the first vibrational states depends on the phase, φ_L. Now we are in a position to guess how wave packets (4) of the harmonic oscillators depend on the phase when $\omega_L = \omega_{10}$

$$|\phi(t)\rangle \approx \sum_{\nu=0}^{\infty}|\nu\rangle c_\nu(t)e^{-i(\nu\varphi_L+\epsilon_\nu t)}, \tag{7}$$

where $c_0(t) \approx 1$, $c_1(t)$ is defined by Eq. (6), and $c_2(t) \sim c_1^2(t)$. The coefficients $c_\nu(t)$ do not depend on φ_L in the rotating wave approximation. Numerical simulations (Fig. 3) which will be discussed in detail in Sec. V show that the trajectory of the center of gravity of the WP

$$\bar{r}(t) = \langle\phi(t)|r|\phi(t)\rangle \tag{8}$$

is very sensitive to the phase of the ir light. Taking into account Fig. 1 it easy to understand that the spectral shape of the x-ray absorption driven by a strong ir radiation depends strongly on the phase.

III. X-RAY PHOTOABSORPTION OF MOLECULES DRIVEN BY A STRONG IR FIELD

We consider the case when a resonant x-ray field excites a molecule from the ground to core-excited electron-

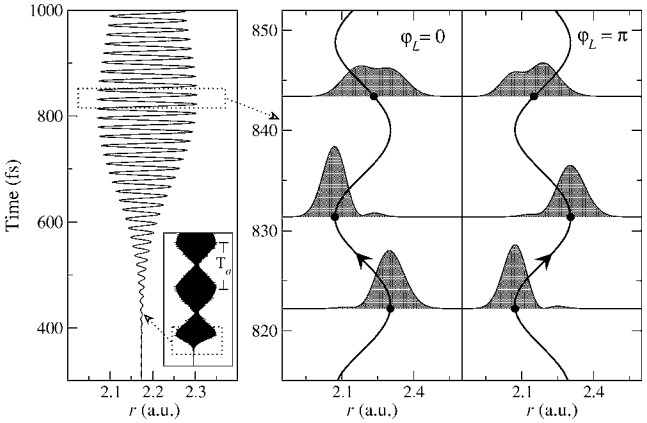

FIG. 3. Trajectory of the WP $\bar{r}(t)$ [Eq. (8)] vs phase of pump field. The case of oriented molecule: $\mathbf{d}\|\mathbf{e}_L$. $I_L=2.3\times10^{12}$ W/cm^2. $\omega_L=\omega_{01}=0.241$ eV. $t_L=700$ fs. $\tau_L=100$ fs. $k_L=1$. Solid lines show the trajectories of the WP. The shaded areas on the right-hand side panel represent wave packets. $T_a\approx1210$ fs.

vibrational states $\psi_0^{\mathrm{el}}\phi(t)\rightarrow\psi_c^{\mathrm{el}}\phi_i(t)$. The population, $\rho_{ii}(t,\Omega)$, of the ith vibrational level of the core-excited state evolves according to the balance equation

$$\left(\frac{\partial}{\partial t}+2\Gamma\right)\rho_{ii}(t,\Omega)=P_i(t,\Omega), \tag{9}$$

where 2Γ is the decay rate of the core-excited state. The total probability of the transitions from ground state to core-excited state

$$P(t,\Omega)=\sum_i P_i(t,\Omega)=-2\,\mathrm{Im}\sum_{i\nu}\rho_{i\nu}(t,\Omega)V_{\nu i}(t) \tag{10}$$

depends on the density matrix of the molecule, $\rho_{ij}(t,\Omega)=a_i(t)a_j^*(t)$, and on the interaction of the molecule with the x-ray pulse, $V_{\nu i}(t)$. Due to near resonant conditions it is possible to use the rotating-wave approximation

$$V_{\nu i}(t)=-\frac{\mathbf{e}\cdot\mathbf{D}_{0c}}{2}E_X(t)\langle\nu|i\rangle e^{i(\Omega-\omega_{i\nu})t+i\varphi_X(t)}. \tag{11}$$

Here $\Omega=\omega_X-\omega_{c0}$ is the detuning of the x-ray field from the resonant frequency of the pure electronic transition $0\rightarrow c$, $\omega_{c0}=E_c(r_e^c)-E_0(r_e^0)$ is the adiabatic excitation energy which constitutes the difference between minima of core excited and ground state potentials, $\omega_{i\nu}=\epsilon_i-\epsilon_\nu$ is the difference between vibrational energies of the core excited and ground states. The x-ray field is assumed to be weak, which means that it does not affect the ground state wave packet (4). In other words, the density matrix element $\rho_{i\nu}(t,\Omega)=a_i(t)a_\nu^*(t)$ in Eq. (10) has the same coefficient $a_\nu(t)$ as the ground state wave packet (4). The amplitude of the ith vibrational level of the core excited state obeys the equation

$$\left(\frac{\partial}{\partial t}+\Gamma\right)a_i(t)=-i\sum_\nu V_{i\nu}(t)a_\nu(t). \tag{12}$$

The substitution of the solution of this equation

$$a_i(t)=i\zeta e^{-\Gamma t}\int_{-\infty}^{t}dt_1E_X(t_1)e^{[-i(\Omega-\epsilon_i)+\Gamma]t_1-i\varphi_X(t_1)}\langle i|\phi(t_1)\rangle,$$

$$\zeta=\frac{1}{2}(\mathbf{e}_X\cdot\mathbf{D}_{c0}) \tag{13}$$

in Eq. (10) results in the following expression for the instantaneous transition probability:

$$P(t,\Omega)=2E_X(t)\,\mathrm{Re}\int_{-\infty}^{t}dt_1E_X(t_1)e^{(i\Omega-\Gamma)(t-t_1)}\Phi(t-t_1)$$
$$\times\langle\phi_c(t)|\phi_c(t_1)\rangle, \tag{14}$$

where

$$|\phi_c(t)\rangle=e^{iH_ct}\zeta|\phi(t)\rangle. \tag{15}$$

Here we introduced the correlation function describing the phase fluctuations of the x-ray field (we ignore the amplitude fluctuations)

$$\Phi(t-t_1)=\langle e^{i[\varphi_X(t)-\varphi_X(t_1)]}\rangle,$$

$$\Phi(\varepsilon)=\frac{1}{2\pi}\int_{-\infty}^{\infty}d\tau\,\Phi(\tau)e^{i\varepsilon\tau}. \tag{16}$$

The angular brackets implicate averaging over the phase fluctuations of the x-ray field. The Fourier transform of the real correlation function, $\Phi(\varepsilon)$, is the spectral function of the x-ray radiation. We assume that the pump field is coherent and has a long correlation time. As it was pointed out above the duration of standard x-ray measurements is longer than the pulse duration. This motivates us to focus attention only on the integral probability

$$P(\Omega)=\int_{-\infty}^{\infty}dtP(t,\Omega)=\int_{-\infty}^{\infty}d\varepsilon\;P_0(\Omega-\varepsilon)K(\varepsilon). \tag{17}$$

Here we introduced the absorption probability for $K(\varepsilon)=\delta(\varepsilon)$

$$P_0(\Omega)=\langle\phi_c(-\Omega)|\phi_c(-\Omega)\rangle \tag{18}$$

and the WP in the frequency domain

$$|\phi_c(-\Omega)\rangle=\int_{-\infty}^{\infty}dt\;e^{-i\Omega t}E_X(t)|\phi_c(t)\rangle. \tag{19}$$

The convolution of the Lorentzian $\Delta(\varepsilon,\Gamma)=\Gamma/[\pi(\varepsilon^2+\Gamma^2)]$, the spectral function of the x-ray field results in the total spectral function

$$K(\varepsilon)=\frac{1}{\pi}\,\mathrm{Re}\int_0^{\infty}d\tau\,\Phi(\tau)e^{-(\Gamma-i\varepsilon)\tau}$$
$$=\int_{-\infty}^{\infty}d\varepsilon_1\Phi(\varepsilon_1)\Delta(\varepsilon_1-\varepsilon,\Gamma). \tag{20}$$

This function becomes a Voigt profile when the spectral function of the x-ray field is a Gaussian.

It is worthwhile to note that the finite duration of the x-ray pulse produces an extra broadening of the spectral lines of

TABLE I. Spectroscopic constants [13] of NO used in the simulations: vibrational frequencies, anharmonicity constants, internuclear distances, probabilities of O $1s\rightarrow 2\pi$ transitions, f.

		Excited States NO*		
Spectral constant	NO $(^2\Pi)$	$(^2\Sigma^-)$	$(^2\Delta)$	$(^2\Sigma^+)$
$\omega_e/\mathrm{cm}^{-1}$	1943.79	1121.11	1282.42	1306.61
$\omega_e x_e/\mathrm{cm}^{-1}$	13.71	9.68	8.87	9.68
$r_e/\text{Å}$	1.146	1.339	1.295	1.290
Γ/eV		0.0870	0.0875	0.0865
$f/f(^2\Sigma^+)$		3.52	2.13	1.00
ω_{c0}/eV		531.30	532.20	533.64

the x-ray absorption. This effect is included in $P_0(\Omega)$ via the amplitude of the x-ray field, $E_X(t)$.

IV. COMPUTATIONAL DETAILS

Our simulations are divided in four blocks: (1) calculation of the nuclear WP $\phi(t)$ in the ground electronic state, solving numerically the Schrödinger equation (5) without any assumption about the intensity of the ir field, (2) evaluation of the nuclear wave packet $\phi_c(t)$ in the potential of the core excited state (15), (3) Fourier transform, $\phi_c(-\Omega)$ (19), of the wave packet $\phi_c(t)$, (4) calculation of the norm $\langle\phi_c(-\Omega)|\phi_c(-\Omega)\rangle$ which is nothing else than the probability of x-ray absorption $P_0(\Omega)$ (18).

To control the contribution of individual vibrational levels in the WP

$$\bar{a}_\nu(t;\varphi_L)=\langle\nu|\phi(t)\rangle,\quad \rho_\nu=|\bar{a}_\nu(t;\varphi_L)|^2 \tag{21}$$

we calculated also the vibrational frequencies and stationary wave functions in the ground electronic state solving the stationary Schrödinger equation: $H_0|\nu\rangle=\epsilon_\nu|\nu\rangle$. Here ρ_ν is the population of the νth vibrational level in the ground electronic state. Both wave packets, $\phi(t)$ and $\phi_c(t)$, are calculated employing time dependent techniques [11] using the ESPEC program [12]. The second order differential scheme is applied in the propagation of the WP with a time step of 5×10^{-5} fs. These parameters preserve the norm of the WP, $\phi(t)$, being equal to one during the propagation.

In the simulations we neglect the lifetime broadening ($\Gamma\approx0.08$ eV) of the core excited state $|\mathrm{O}\ 1s\rightarrow2\pi\rangle$ of the NO molecule (except Sec. V B), as well as the broadening due to the spectral function of the x-ray field, $\Phi(\varepsilon)$. This is a reasonable approximation considering that the rather short x-ray pulses using $\tau_X\approx3-20$ fs give quite large spectral broadening $1/\tau_L\approx0.5-0.07$ eV.

The propagation of the WPs is calculated using computed Morse potentials [13] for the core excited $(^2\Sigma^-)$ $1\sigma^12\sigma^23\sigma^24\sigma^21\pi^45\sigma^22\pi^2$ and ground $(^2\Pi)$ $1\sigma^22\sigma^23\sigma^24\sigma^21\pi^45\sigma^22\pi^1$ states of the NO molecule. The detuning of the x-ray field $\Omega=\omega-\omega_{c0}$ is defined relative to the adiabatic excitation energy [13] $\omega_{c0}=531.3$ eV. The other parameters of the Morse potential are listed in Table I. The potential energy curve is mapped from 0.5 until 2.8 Å with 256 points. It is noteworthy that the strong pump field can mix different electronic states and, hence it can change the molecular potential [14,15]. This effect is neglected here because it is small for the NO molecule, with large spacing between first excited and ground electronic states, >5 eV [16].

The dynamics of the ground state wave packet $\phi(t)$ (5) is simulated using an r-dependent dipole moment $d=d(r)$ (Fig. 4), which was computed by the CAS-MCSCF method with DALTON [17]. The active space is formed by 11 electrons in 10 orbitals comprising the nitrogen and oxygen second shell. The N K and O K electrons are kept inactive. Two different basis sets are used in the calculations, aug-cc-pVDZ and aug-cc-pVTZ, giving quite similar results (see Fig. 4). As one can see from Table II the r-dependence of this dipole moment results in a rather weak breakdown of the dipole selection rules. The r-dependence of the transition dipole moment of the core excitation D_{c0} is neglected. This is a good approximation due to the strong localization of the O $1s$ orbital.

We have used the following relation between parameters in atomic units and in SI units: $dE[\text{a.u.}]=d[\text{D}]\times\sqrt{I[\mathrm{W/cm}^2]}\times2.1132\times10^{-9}$ a.u., $\Omega t[\text{a.u.}]=\Omega(\text{a.u.})\times t(\text{fs})\times41.3417$. Here $I=c\varepsilon_0|E(t)|^2/2$ is the intensity of radiation. The ir radiation is assumed to be in resonance with the first vibrational transition, $\omega_L=\omega_{10}$, everywhere except for the situation depicted in Fig. 9 where $\omega_L=\omega_{20}$.

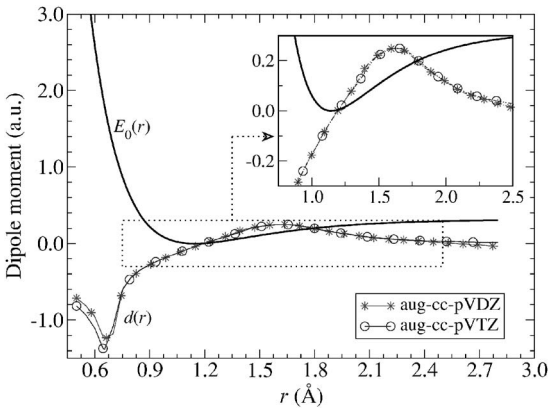

FIG. 4. Dependence of permanent dipole moment, $d(r)$, of nitrogen monoxide molecule in ground state on the internuclear distance, r. Both dipole moment and ground state energy $[E_0(r)]$ are in a.u.

TABLE II. Dipole moments $d_{\nu\nu'}$ of ir transitions in the ground state of the NO molecule (in D).

$\nu \to \nu'$	$d_{\nu\nu'}$	$\nu \to \nu'$	$d_{\nu\nu'}$	$\nu \to \nu'$	$d_{\nu\nu'}$
$0 \to 1$	0.07284	$1 \to 2$	0.10271	$2 \to 4$	0.01476
$0 \to 2$	0.00615	$1 \to 3$	0.01056	$2 \to 5$	0.00264
$0 \to 3$	0.00076	$1 \to 4$	0.00156	$3 \to 4$	0.14488
$0 \to 4$	0.00008	$1 \to 5$	0.00018	$3 \to 5$	0.01863
$0 \to 5$	0.00001	$2 \to 3$	0.12552	$4 \to 5$	0.16224

The temporal shape of the ir and x-ray pulses is modeled in the calculations as follows:

$$I_\alpha \exp\left[-\left(\frac{t-t_\alpha}{\bar{\tau}_\alpha}\right)^{2k_\alpha}\right], \quad \bar{\tau}_\alpha = \frac{\tau_\alpha}{(\ln 2)^{1/2k_\alpha}}, \tag{22}$$

where τ_α is the half width at half maximum (HWHM), $k_\alpha = 1, 2, \ldots$. This expression is convenient because it describes a smooth transition from a Gaussian ($k=1$) to a rectangular function ($k \gg 1$). In the simulations we used the Gaussian shape ($k=1$) of the pump and probe pulses and assumed the following values for the peak position ($t_L = 700$ fs) and the duration ($\tau_L = 100$ fs) of the pump pulse [except Fig. 7(b)]. Through all calculations it is assumed that the x-ray pulse probes the system after the ir pulse leaves it: $\Delta t > 2(\tau_L + \tau_X)$. Everywhere except for the cases reproduced in Figs. 8 and 9 our simulations were performed for oriented NO molecules: $\mathbf{d} \| \mathbf{e}_L$.

V. RESULTS

A. Gross spectral features

It is instructive to start analyzing the gross spectral features of the x-ray pump-probe spectra. Throughout the paper we focus our attention only on the x-ray transition $^2\Pi \to {}^2\Sigma^-$ in NO, except in Sec. V B. The reference spectrum is the ordinary x-ray absorption profile of NO without ir field (spectrum A in Fig. 1). The spectrum changes qualitatively if the molecule is exposed to a strong ir field. Due to the r-dependence of the permanent dipole moment $d(r)$ (Fig. 1), the ir field populates higher vibrational levels of the ground state and creates a coherent superposition, $\phi(t)$. The WP performs back and forth oscillations in the ground state potential. The time dependence of the peak position, r, of $\phi(t)$ affects the probe spectrum measured at a certain instant. When the x-ray pulse is short ($\tau_X = 3$ fs) the proper choice of the delay time, $\Delta t = t_X - t_L$ (or ir phase), allows one to get a snapshot of the x-ray spectra for WPs localized near the left (B) or right (C) turning points. The B and C spectra (Fig. 1) differ qualitatively because their vertical transitions have different energies. The x-ray spectrum is approximately the sum of spectra B and C if the duration of the x-ray pulse is longer or comparable with the period of oscillations of the wave packet: $\tau_X \gtrsim 2\pi/\omega_{10} \approx 17$ fs (see spectrum D in Fig. 1). This is because the WP has time to move from left to right turning points in this case. When the probe and pump pulses overlap the x-ray spectrum depends on the delay time both for short and long pulses due to the sensitivity of the populations of vibrational levels to Δt. When the ir pulse leaves the system the x-ray spectrum continues to depend on Δt if the x-ray pulse is short; when the x-ray pulse is long the spectrum ceases to depend on the delay time (see Sec. V F).

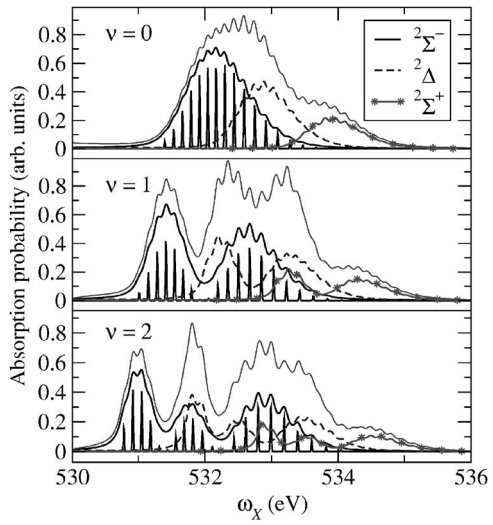

FIG. 5. The partial O K x-ray absorption profiles $P^{(\nu)}(\Omega)$ [Eq. (24)] of NO excited in ground state vibrational levels $\nu = 0, 1, 2$ for different core-excited states: $^2\Sigma^-$, $^2\Delta$, and $^2\Sigma^+$. The total spectral profiles are shown by the thin solid lines. Narrow resonances display the spectral distribution of the Franck-Condon factors for the $^2\Sigma^-$ core-excited state.

It is worthwhile to note that the ir field changes the mean vibrational energy of the ground state

$$\Delta\epsilon = \epsilon(t) - \epsilon_0, \quad \epsilon(t) = \langle \phi(t) | H_0 | \phi(t) \rangle. \tag{23}$$

This results in a shift of the center of gravity of the x-ray spectrum. In the general case this shift depends on the delay time and the intensity of the ir pulse. Such a shift, $\Delta\epsilon \approx 0.23$ eV, is shown in Fig. 1 for $\Delta t > 2(\tau_L + \tau_X)$ when $\Delta\epsilon$ ceases to depend on the delay time. The ir intensity affects the x-ray spectrum because a larger $\Delta\epsilon$ corresponds to a larger distance between the left and right turning points of the wave packet in the potential (see Fig. 1).

The influence of the x-ray pulse duration on the spectral resolution deserves a short remark. When the x-ray pulse is rather long ($\tau_X \gtrsim 2\pi/\omega_{10} \approx 17$ fs), the spectra display vibrational structure (see the spectra A and D in Fig. 1), while the vibrational resolution is washed out if the x-ray pulse is short (Fig. 1 spectra B and C) because of the uncertainty relation between time and energy.

B. X-ray absorption of NO molecules in the field of incoherent pump radiation

The molecule is excited from lowest to higher vibrational levels by the strong ir field. Such an excitation influences the x-ray absorption due to the change of the populations of vibrational states as well as due to the coherence between these states created by the ir field (see Sec. II B). We consider in this section the incoherent ir pulse with randomly fluctuating phase, $\varphi_L(t)$. Due to this randomness the coherence between different vibrational states of the WP, $\phi(t)$ [Eq. (7)], is destroyed and the x-ray absorption probability becomes a simple sum of partial contributions

$$P(\Omega) = \sum_{\nu} \rho_{\nu} P^{(\nu)}(\Omega). \tag{24}$$

Here $P^{(\nu)}(\Omega)$ is the probability of x-ray transition from vibrational level ν with the population ρ_{ν} [Eq. (21)]. Figure 5 shows the partial x-ray spectra, $P^{(\nu)}(\Omega)$, of O $1s \rightarrow 2\pi$ absorption for three different initial vibrational states, $\nu = 0, 1, 2$. In this figure we show the total and partial absorption spectra which correspond to the core-excitation in different close-lying final states [13], $^2\Sigma^-$, $^2\Delta$, and $^2\Sigma^+$. The spectroscopic parameters used in the simulations are collected in Table I. One can see that the different initial vibrational states result in very different x-ray spectra, something that can be referred to the different distributions of the Franck-Condon factors, $\langle 0|i\rangle^2$, $\langle 1|i\rangle^2$, and $\langle 2|i\rangle^2$ and the quite large displacement of the potential well of the core-excited state relative to the ground state potential.

Apparently, the x-ray absorption of NO driven by an incoherent pump field (24) does not depend on the phase φ_L due to phase independence of the populations ρ_{ν} (Fig. 5). However, the x-ray spectrum is sensitive to the delay time because of the time dependence of populations. Such a time dependence takes place in the studied case only when the x-ray pulse overlaps with the ir incoherent pulse.

Let us now investigate ir–x-ray pump probe spectroscopy in the field of coherent ir radiation [see Eq. (18)]. In order to focus our attention on the physics we will only study the x-ray absorption band related to the lowest final state $^2\Sigma^-$.

C. Dynamics of the nuclear wave packet versus phase and Rabi oscillations. Phase memory versus the shape of the pulse

The coherent pump field prepares the wave packet $\phi(t)$ which is probed by the x-ray pulse. We have shown in Sec. II B that the WP and, hence, the x-ray absorption is sensitive to the phase of the strong ir field, φ_L. The simulations indicate a strong dependence of the trajectory of the wave packet on the phase, Fig. 3. As one can see from this figure the WP performs fast back and forth oscillations with the vibrational frequency ω_{10}, and is modulated with a lower frequency: $\Delta\omega_a = \omega_{10} - \omega_{21} = 2\omega_e x_e = 2 \times 13.71$ cm^{-1} (see Table I). This modulation caused by the anharmonicity of the ground state potential has the period $T_a = 2\pi/\Delta\omega_a \approx 1210$ fs (see inset of Fig. 3). One can show that the trajectories of the center of gravity of the x-ray spectrum and of the wave packet are quite similar [18]. The measurement of the time interval between the adjacent nodes of the trajectory gives directly the revival time, T_a. This allows one to measure the anharmonicity constant.

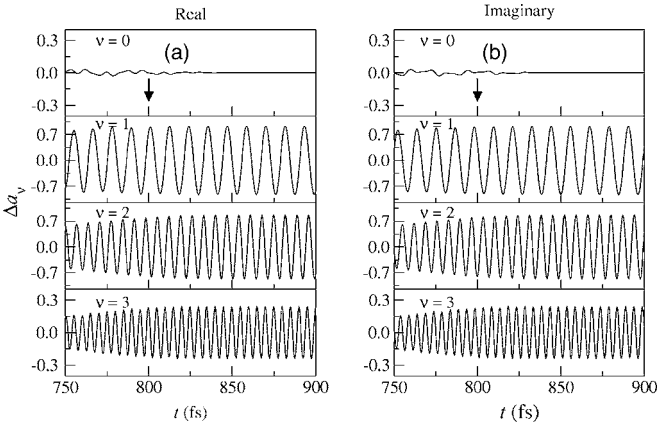

FIG. 6. The phase dependence of the contributions $\tilde{a}_{\nu}$ (21) of different vibrational states ($\nu = 0, 1, 2, 3$) in the wave packet, $\phi(t)$: $\Delta a_{\nu} = \tilde{a}_{\nu}(\varphi_L = 0) - \tilde{a}_{\nu}(\varphi_L = \pi/2)$. The left and right panels show the real and imaginary part of Δa_{ν}. $I_L = 2.3 \times 10^{12}$ W/cm^2. $\omega_L = \omega_{01} = 0.241$ eV. $t_L = 700$ fs. $\tau_L = 100$ fs. $k_L = 1$. The vertical arrows shows the instant where the ir intensity is decreased in two times.

The phase effect can be explained also with help of classical mechanics. According to Ehrenfest's theorem the mean value of the force which affects the center of gravity of the wave packet

$$\langle F \rangle = \langle \phi(t) | \frac{d}{dr} [\mathbf{E}_L(t) \cdot \mathbf{d}(r)] \cos(\omega_L t + \varphi_L) | \phi(t) \rangle$$

depends on the ir phase, φ_L. For example, this force changes the sign when $\varphi_L \rightarrow \varphi_L + \pi$. This means that the evolution of the WP in the potential well depends on the phase.

The phase sensitivity is clearly seen from the strong phase dependence in the projections of the WP on the stationary vibrational state, $\tilde{a}_{\nu}$ (21) which was calculated for $\varphi_L = 0$ and $\varphi_L = \pi/2$ (see Fig. 6). The simulations are in nice agreement with the simple equation (7)

$$\tilde{a}_{\nu} \sim e^{-i(\nu\varphi_L + \epsilon_{\nu} t)}, \quad \nu = 0, 1.2, \ldots, \tag{25}$$

which is valid for $\omega_L = \omega_{10}$. According to this equation the amplitude of the lowest vibrational level, $\tilde{a}_0$, does not depend on the phase. The simulations display very weak phase dependence of $\tilde{a}_0$ which, probably, is due to the slight break down of the rotating wave approximation which is used in Eqs. (7) and (25), while the amplitudes of higher vibrational levels of $\tilde{a}_1$, $\tilde{a}_2$, and $\tilde{a}_3$ strongly depend on the phase (Fig. 6). Equation (25) indicates that $\tilde{a}_{\nu}$ oscillates with the period $T_{\nu} = 2\pi/\epsilon_{\nu}$, for example, $T_1 = 11.56$ fs, $T_2 = 6.98$ fs, and $T_3 = 5.03$ fs. These values agree perfectly with the simulations based on the strict solution of the Schrödinger equation (5) (see Fig. 6). It can be also seen in Fig. 6 that the amplitudes $\tilde{a}_{\nu}$ and, hence the wave packet $\phi(t)$ depend on the phase φ_L during the interaction with the pump pulse, as well as later when the pulse leaves the system. The main reason for such a long memory about the phase is the long lifetime of the vibrational levels of the ground state (this time is assumed to

be infinite in our simulations). Clearly, the x-ray spectrum also keeps the phase memory when the pump pulse leaves the system.

Contrary to the real and imaginary parts of $\tilde{a}_\nu$, the populations of vibrational levels $\rho_\nu=|\tilde{a}_\nu|^2$ (21) almost do not depend on the phase. Figure 7(a) shows only a weak modulation of ρ_ν

$$\frac{\delta\rho_\nu}{\rho_\nu} \sim \frac{G_R}{\omega_L}\cos(2\omega_L t + 2\varphi_L) \tag{26}$$

with twice the frequency of the ir field. These oscillations origin in the off-resonant interaction with the field and they depend on the phase φ_L. The inset in Fig. 7(a) displays different time dependences for $\varphi_L=0$ and $\varphi_L=\pi/2$. Simulations show that the phase $\varphi_L=\pi$ gives the same results as $\varphi_L=0$ in agreement with Eq. (26). The off-resonant interaction can be important when the Rabi frequency,

$$G_R=|\mathbf{E}_L\cdot\mathbf{d}_{10}|, \quad T_R=\frac{2\pi}{G_R}, \tag{27}$$

approaches the ir frequency, ω_L (when the rotating wave approximation breaks down). Evidence that the weak modulation of the populations with the frequency $2\omega_L$ are related to the Rabi frequency is given by the absence of these oscillations in the region where the ir intensity is very low [Fig. 7(a)].

The ir intensity used in the simulations shown in Fig. 7 corresponds to the Rabi period (27) around 750 fs which is longer than the duration of the ir pulse, $\tau_L=100$ fs. This corresponds to the limiting case of a sudden switching of the pump field: The ir field is shut off faster than the Rabi period and the molecule remains in the vibrationally excited state after the pulse leaves the system [Fig. 7(a)] which then keeps the phase memory. The scenario changes drastically when the time for the switching-off of the ir pulse, $\Delta T\approx 715$ fs, is long and becomes comparable with the Rabi period, $T_R\approx 750$ fs [see Fig. 7(b)]. In this case the field is shut off slowly and the system follows adiabatically the slow decrease of the light intensity up to zero where only the lowest vibrational level is populated [Fig. 7(b)]. In this case the phase will influence the x-ray spectrum only when the x-ray and pump pulses overlap in the time domain. The phase sensitivity is absent when the x-ray pulse exposes the molecules after the ir pulse leaves the system; moreover, the x-ray spectrum coincides, in this case, with the x-ray spectrum of the molecules without the ir field. So in the adiabatic limit, $\Delta T \gtrsim T_R$, any memory about the ir pulse is absent.

D. Influence of the phase of the ir field on x-ray absorption by oriented molecules

The phase of the ir field strongly influences the shape of x-ray absorption. This is seen clearly from Figs. 8 and 9 where the x-ray absorption probabilities are shown for four different phases, $\varphi_L=0$, $\pi/2$, π, and $3\pi/2$. The physical mechanism of such a phase sensitivity, described in Sec. II is directly related to the phase dependence of the dynamics of the WP. It is important to note here that the x-ray pulse

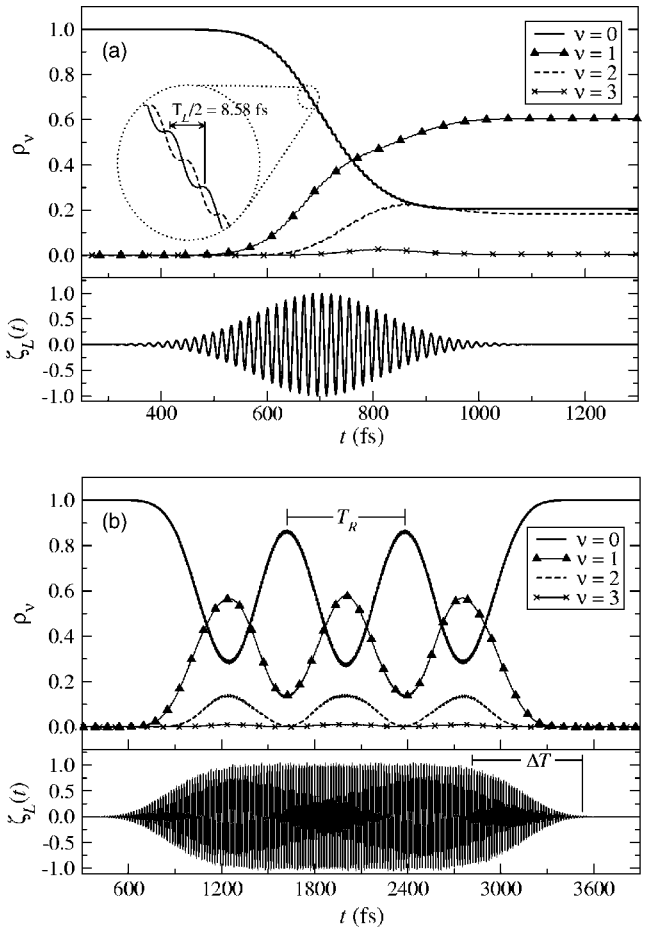

FIG. 7. Populations, ρ_ν [Eq. (21)] of the vibrational levels of the ground electronic state vs time for different durations of switching off the pump field [which is $\tau_L=100$ fs for short pulse (a), and $\Delta T\approx 715$ fs for long rectangular pulse (b)]. $\zeta_L(t)=\mathcal{E}_L(t)/\mathcal{E}_L^{\max}(t)=\sqrt{\Phi_L(t-t_L)}\cos(\omega_L t)$ is the time distribution of the pump field with the peak value normalized to one [see Eq. (22)]. $\omega_L=\omega_{01}=0.241$ eV. $I_L=2.3\times10^{12}$ W/cm^2. $\varphi_L=0$. (a) $t_L=700$ fs, $\tau_L=100$ fs. $k_L=1$. The inset shows the case $\varphi_L=\pi/2$. (b) $t_L=2$ ps, $\tau_L=1$ ps. $k_L=3$.

probes the system after the pump pulse leaves the system. Thus both Figs. 8 and 9 evidence the above discussed effect of the phase memory.

Figures 8(a) and 8(b) show x-ray spectra when $\Omega_L=\omega_{10}=0.241$ eV for two different ir intensities, 1.5×10^{12} and 2.3×10^{12} W/cm^2, respectively. The weaker pump field populates mainly the two first vibrational states and creates the following distribution of vibrational populations; $\rho_0=0.374$, $\rho_1=0.527$, $\rho_2=0.097$, $\rho_3=0.002$. The population distribution in the stronger ir field, $\rho_0=0.208$, $\rho_1=0.605$, $\rho_2=0.182$, $\rho_3=0.005$, shows the population of the level, $\nu=2$, also. The phase influence is strong in both cases. However, we see below that the population of level $\nu=2$ becomes very important for randomly oriented molecules. Let us note that the transition energy is influenced also by the mean energy of the wave packet $\varepsilon(t)$ [Eq. (23)]. This energy depends on the time when the ir pulse interacts with the molecule and it is time-independent when the pulse leaves the system. After the pump pulse leaves, $\varepsilon(t)=0.29$ and 0.35 eV for the param-

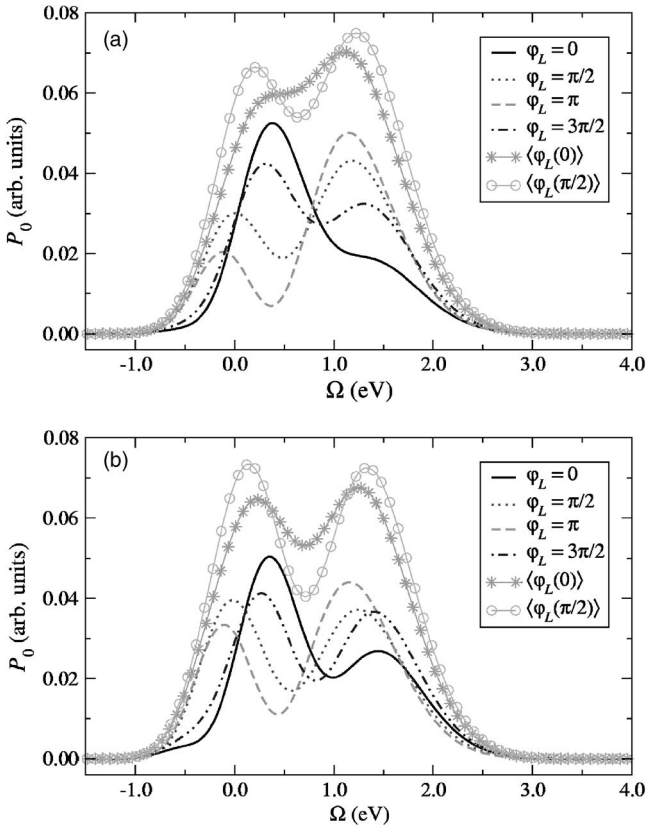

FIG. 8. Phase dependence of the probability of O K x-ray absorption of NO [Eq. (18)]. The frequency of the ir field is tuned in resonance with the first vibrational level: $\omega_L=\omega_{01}=0.241$ eV. The spectra averaged over molecular orientations (29) are marked by $\langle\varphi_L\rangle$ with $\varphi_L=0$ and $\pi/2$. $\tau_X=3$ fs. The delay time: $\Delta t=610$ fs. $\Omega=\omega-531.3$ eV. (a) $I_L=1.5\times10^{12}$ W/cm^2. (b) $I_L=2.3\times10^{12}$ W/cm^2.

eters used in Figs. 8(a) and 8(b), respectively.

When the pump field is tuned in resonance with the second vibrational level, $\Omega_L=\omega_{20}=0.4717$ eV, the efficiency of the population decreases strongly because the corresponding transition dipole moment, being proportional to $\langle 0|d(r)|2\rangle \approx d''\langle 0|r^2|2\rangle$, is small. In order to populate the higher vibrational levels an ir intensity of $I_L=3.0966\times10^{13}$ W/cm^2 was used. In this case it only populates efficiently the ground state and the second vibrational level ($\nu=2$): $\rho_0=0.817$, $\rho_1=0.000$, $\rho_2=0.182$, and $\rho_3=0.001$. The mean energy of the wave packet is in this case $\varepsilon(t)=0.21$ eV. Here and above the populations as well as $\varepsilon(t)$ correspond to times after that the ir pulse left the system.

E. Probe signal from randomly oriented molecules and nonlinearity

Usually molecules are randomly oriented and the probe signal (18) has to be averaged over molecular orientations. The orientational averaging strongly affects the phase dependence which origins in the interference term (3). When the pump intensity is weak, the ir field populates only the first vibrational levels, $\nu=1$. In this case the interference term is equal to zero

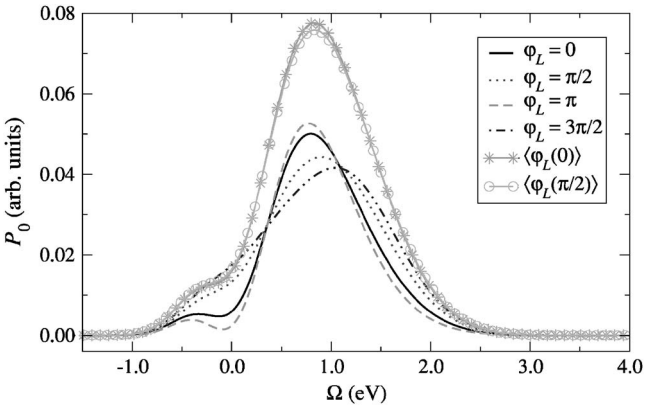

FIG. 9. Phase dependence of the probability of O K x-ray absorption of NO [Eq. (18)]. The frequency of the pump is tuned in resonance with the second vibrational level: $\omega_L=\omega_{02}=0.4717$ eV. $I_L=3.0966\times10^{13}$ W/cm^2. The other parameters are the same as in Fig. 8.

$$\overline{P_{\rm int}^{(1)}(t)} \propto \overline{(\mathbf{d}_{10}\cdot\mathbf{e}_L)|\mathbf{D}_{c0}\cdot\mathbf{e}_X|^2}=0 \qquad (28)$$

and the phase dependence is absent. Such a quenching of the interference is due to that the two opposite molecular orientations, $\mathbf{d}_{10}$ and $-\mathbf{d}_{10}$, cancel each other. As one can see from Eq. (1) the change of the sign $(\mathbf{d}_{10}\cdot\mathbf{e}_L)$ is equivalent to the change of the phase $\varphi_L\rightarrow\varphi_L+\pi$. We performed orientational averaging taking only into account the most important molecular orientations, namely the two opposite orientations:

$$\bar{P}_0(\omega,\varphi_L)\approx\frac{1}{2}[P_0(\omega,\varphi_L)+P_0(\omega,\varphi_L+\pi)]. \qquad (29)$$

The x-ray spectra averaged over molecular orientations are marked in Figs. 8 and 9 as $\langle\varphi_L\rangle$. Figure 8 (compare spectra $\langle 0\rangle$ and $\langle\pi/2\rangle$) displays a suppression of the phase effect for the ir intensity 1.5×10^{12} W/cm^2 and a strong phase dependence for higher intensity, $I_L=2.3\times10^{12}$ W/cm^2. Mainly levels $\nu=0$ and 1 are populated in the first case: $\rho_0=0.374$, $\rho_1=0.527$, and $\rho_2=0.097$. Equation (28) explains the small phase effect for randomly oriented molecules in such a field. For higher intensity, 2.3×10^{12} W/cm^2, the level $\nu=2$ is higher populated: $\rho_0=0.208$, $\rho_1=0.605$, $\rho_2=0.182$, and $\rho_3=0.005$. This results in a nonzero interference term (3):

$$\overline{P_{\rm int}^{(2)}(t)} \propto \overline{|\mathbf{d}_{10}\cdot\mathbf{e}_L|^2|\mathbf{D}_{c0}\cdot\mathbf{e}_X|^2}\neq 0.$$

Figure 9 indicates a strong suppression of the phase dependence when the ir frequency is tuned in resonance with the transition $0\rightarrow2$. The reason for this is the small value of the transition dipole moment $\mathbf{d}_{20}$ which suppresses the population of higher vibrational levels, $\nu\geqslant3$. In this case mainly the one-photon channel $0\rightarrow2$ influences x-ray absorption and the interference term similar to Eq. (28) is quenched: $\overline{(\mathbf{d}_{20}\cdot\mathbf{e}_L)|\mathbf{D}_{c0}\cdot\mathbf{e}_X|^2}=0$.

F. Phase effect versus x-ray frequency, duration of x-ray pulse, and delay time

Any phase effect is related to interference. In our case the interference operates between one- and many-photon absorp-

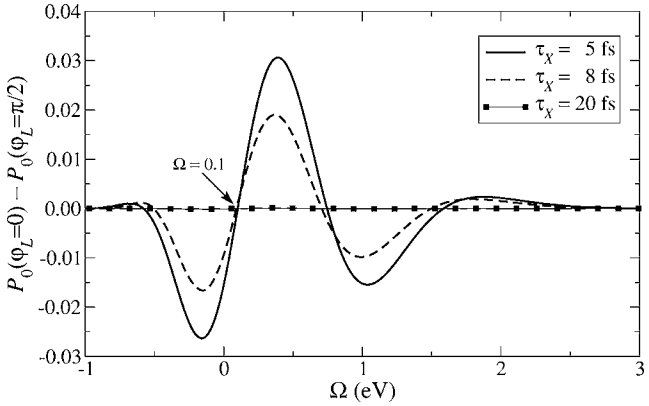

FIG. 10. Difference between x-ray absorption spectra (18) for $\varphi_L=0$ and $\varphi_L=\pi/2$. 2.3×10^{12} W/cm^2. Delay time is $\Delta t=610$ fs.

tion channels. The contributions of these different channels strongly depend on the frequency of the x-ray field, ω_X. This means that the interference, as well as the phase effect, are different for different ω_X, something that is clearly illustrated in Fig. 10.

We already recognized (Fig. 2) that the phase of the pump field influences the x-ray spectrum when $\tau_X \lesssim \pi/\omega_{10}$ =8.58 fs. This simple estimate is in accord with results of the strict simulations, Figs. 10 and 11, which show that the phase dependence decreases for $\tau_X \gtrsim 5$ fs. It is interesting that the phase effect also vanishes for small durations of the x-ray pulse. The short x-ray pulse has many harmonics with different frequencies, ω_X. Thus to understand what is going on with the probe signal for shorter pulses we have to convolute the probe spectrum Fig. 8 with the spectral distribution with

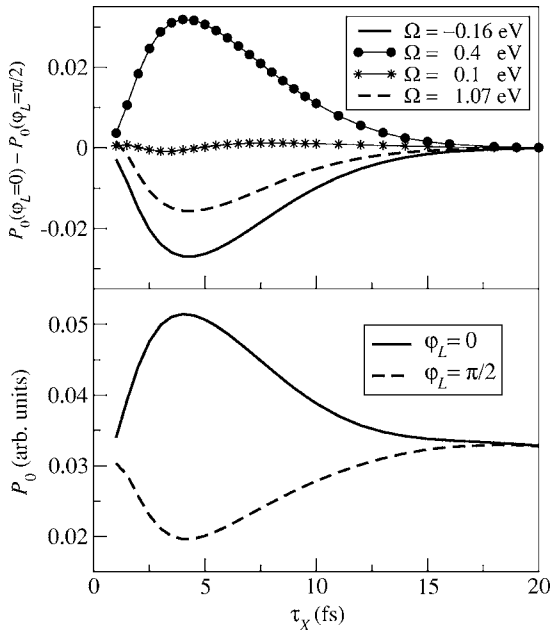

FIG. 11. Probability of x-ray absorption (O $1s\rightarrow 2\pi$) of NO vs duration of x-ray pulse, τ_X for different phases (lower panel). Upper panel displays the phase dependence for different Ω. $I_L=2.3\times10^{12}$ W/cm^2, delay time $\Delta t=610$ fs. Ω=0.4 eV in the lower panel.

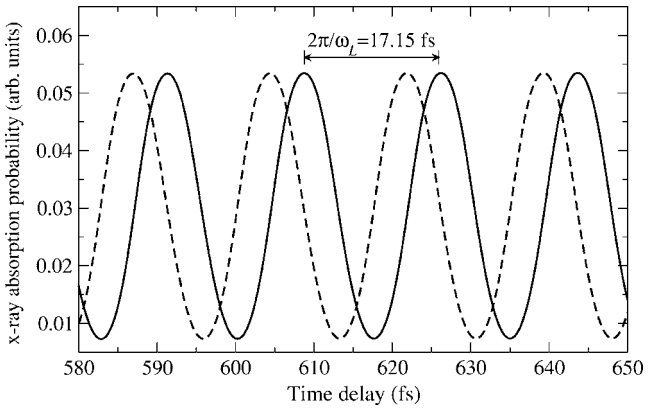

FIG. 12. Probability of x-ray absorption (O $1s\rightarrow 2\pi$) of NO [Eq. (18)] vs delay time, $\Delta t=t_X-t_L$, and the phase of ir field, φ_L. Solid line: $\varphi_L=0$. Broken line: $\varphi_L=\pi/2$. τ_X=4 fs. Ω=0.4 eV. $\omega_L=\omega_{10}$=0.241 eV. $I_L=2.3\times10^{12}$ W/cm^2. t_L=700 fs. τ_L=100 fs.

the width $\sim 1/\tau_X$. As one can see from Fig. 8 such a convolution diminishes the difference between x-ray spectra for different phases if τ_X is small. The phase effect takes maximum value when $\tau_X \approx T_L/4$.

Figure 12 shows the dependence of x-ray absorption on the delay time for two different phases: $\varphi_L=0, \pi/2$. The results of simulations presented here confirm perfectly the qualitative picture, Fig. 2. Figure 12 says that the phase and the delay time play a similar role.

VI. POSSIBILITY OF EXPERIMENTAL OBSERVATIONS

A few words about the possibility of experimental observation of the phase sensitivity of x-ray absorption are in place. First of all, our simulations are performed for a real molecular system and from this point of view our predictions operate with realistic quantities. An intensity of the ir pulse around 10^{12} W/cm^2 is sufficient to populate the first vibrational levels and to see the phase effect. This means that the intensity of the x-ray pulse is the same as is used in standard x-ray absorption measurements. From this point of view one can use conventional synchrotron radiation light sources.

The main problem which we face now is the duration of the x-ray pulse. To observe the discussed phase effect this duration time must be comparable with the period of the vibrational mode. For the NO molecule the duration must be around $\tau_X \sim 5-10$ fs. This requirement can be weaker for polyatomic or heavy molecules which have much smaller vibrational frequencies. This makes the duration essentially longer, $\tau_X \sim 100$ fs. Already now ultrashort x-ray pulses generated by high harmonics with $\tau_X \sim 1$ fs are available [2]. The current state of affairs for creation of short x-ray pulses was overviewed briefly in Ref. [1].

As shown above, a rather strong ir pulse, $\sim 10^{12}$ W/cm^2, is needed to create a nuclear wave packet. Tunable wavelengths in the range from 1 up to 20 μm can be produced via optical parametric amplification or via the second harmonic generation of a 10.6 μm CO_2 laser [19]. The desired intensity, $\approx 10^{12}$ W/cm^2, can be obtained by tight focusing of the light beam in the spot with appropriate diameter. It is worth

mentioning that many other molecular systems have different vibrational frequencies, which match properly with available ir or mid ir powerful lasers. Some of these molecules can be resonantly excited by ir pulses with the wavelength $\sim 10.6\ \mu$m (CO_2 laser) or by ~ 1064 nm (Nd:YAG laser [20]) or by lasers produced using the technique of chirped pulse amplification (CPA), which is an extremely promising tool to generate powerful lasers. An advantage of the optical parametric amplification over the CPA technique is to allow the study of several different molecular systems, due to its intrinsic tunability via phase matching in the nonlinear crystal. Commercial lasers [21] exist which generate about 10 μJ, 30 fs pulses at $1-10\ \mu$m. Another advantage is that such pulses are automatically locked in time to a powerful titanium-sapphire pump, which in principle is able to produce x-ray radiation via high order harmonic generation.

We have shown that the phase effect can be observed both for oriented and disordered molecules. In the first case the effect is stronger. Fortunately, there exist powerful techniques to measure x-ray absorption from fixed-in-space molecules in coincidence experiments applied on randomly oriented molecules [22–24]. Let us mention also the possibility of alignment and orientation of the molecules by a strong ir field [25,26].

VII. SUMMARY

In this work we have theoretically predicted different x-ray absorption spectra of the NO molecule driven by a strong ir field. The x-ray absorption excited incoherently in different vibrational levels of the ground state was found to demonstrate a strong dependence of the absorption profile on the initial vibrational state and on the final electronic state. Special attention was paid on the coherent superposition of ground state vibrational levels created by an ir laser. In this case the simulations displayed a strong dependence of the trajectory of the vibrational wave packet on the phase of the ir field. The trajectory of the wave packet experiences oscillations in the potential well with two qualitatively different frequencies. The wave packet performs fast back and forth oscillations with the vibrational frequency but which are modulated by the anharmonicity of the potential. This fact allows in principle one to measure the anharmonicity constant through the revival time of the center of gravity of the x-ray spectrum.

The phase sensitivity of the trajectory results in a dependence of the x-ray absorption profile on the phase and delay time. The x-ray absorption profile displays a maximum interference pattern when the duration of the probe x-ray pulse is one-fourth of the infrared field period. There is here an important distinction from standard few-cycle optical experiments, namely that in our case the duration of both pump and probe pulses are longer than the inverse frequencies of the corresponding fields. The phase effect is found to be sensitive to the duration of the x-ray pulse. We have found a phase memory effect, namely that the x-ray spectrum keeps the memory about the phase after the ir pulse leaves the system. Such a phase memory strongly depends on the relation between the time of switching-off the ir pulse and the Rabi frequency.

We have shown that when the pump field is weak its phase does not influence the x-ray absorption if the molecules are randomly oriented. In this case the discussed interference effect can be observed only for oriented molecules. One can accomplish orientation by making use of surface adsorbed molecules or by detection of x-ray absorption in the ion yield mode. The interference pattern for randomly oriented molecules starts to grow when the intensity of the pump radiation increases and the pump field is able to populate even vibrational levels. Thus a third way to detect the phase sensitivity of the x-ray absorption of disordered molecules is to use rather high intensities of the pump field. In that case the interference between the different photon excitation channels can be enhanced controlling the intensity and time duration of the infrared pulse.

ACKNOWLEDGMENTS

This work was supported by the Swedish Research Council (VR) and by the STINT foundation. V.C.F. and F.F.G. acknowledge financial support from Conselho Nacional de Desenvolvimento Científico e Tecnológico (CNPq) and Coordenação de Aperfeiçoamento de Pessoal de Nível Superior (CAPES) (Brazil). F.G. acknowledge also financial support from the Russian Foundation for Basic Research (Project No. 04-02-81020-Bel 2004). We acknowledge Professor Michael Meyer for fruitful discussions of current and future possibilities of experimental measurements of the phase effect.

[1] V. C. Felicíssimo, F. F. Guimarães, F. Gel'mukhanov, A. Cesar, and H. Ågren, J. Chem. Phys. **122**, 094319 (2005).
[2] R. Kienberger, E. Goulielmakis, M. Uiberacker, A. Baltuska, V. Yakovlev, F. Bammer, A. Scrinzi, Th. Westerwalbesloh, U. Kleineberg, U. Heinzmann, M. Drescher, and F. Krausz, Nature (London) **427**, 817 (2004).
[3] B. W. Adams, Rev. Sci. Instrum. **75**, 1982 (2004).
[4] R. W. Schoenlein, W. P. Leemans, A. H. Chin, P. Volfbeyn, T. E. Glover, P. Balling, M. Zolotorev, K. J. Kim, S. Chattopadhyay, and C. V. Shank, Science **274**, 236 (1996).
[5] R. W. Schoenlein, S. Chattopadhyay, H. H. W. Chong, T. E. Glover, P. A. Heimann, W. P. Leemans, C. V. Shank, A. A. Zholents, and M. Zolotorev, Appl. Phys. B: Lasers Opt. **71**, 1 (2000).
[6] A. A. Zholents and W. M. Fawley, Phys. Rev. Lett. **92**, 224801 (2004).
[7] T. Brabec and F. Krausz, Rev. Mod. Phys. **72**, 545 (2000).
[8] A. Apolonski *et al.*, Phys. Rev. Lett. **92**, 073902 (2004).
[9] S. Chelkowski, A. D. Bandrauk, and A. Apolonski, Opt. Lett. **29**, 1557 (2004).
[10] F. F. Guimarães, V. Kimberg, F. Gel'mukhanov and H. Ågren, Phys. Rev. A **70**, 062504 (2004).

[11] C. Leforestier *et al.*, J. Comput. Phys. **94**, 59 (1991).
[12] F. F. Guimarães, V. C. Felicíssimo, V. Kimberg, A. Cesar, and F. Gel'mukhanov, *eSPec wave packet propagation program*, Universidade Federal de Minas Gerais, Brazil and Royal Institute of Technology, Sweden, 2004, see http://www.theochem.kth.se/people/freddy/.
[13] R. Fink, J. Chem. Phys. **106**, 4038 (1997).
[14] A. D. Bandrauk, E. Aubanel, and J.-M. Gauthier, in *Molecules in Laser Fields*, edited by A. D. Bandrauk (Marcel Dekker, New York, 1994), Chap. 3.
[15] C. Wunderlich, E. Kobler, H. Figger and Th. W. Hänsch, Phys. Rev. Lett. **78**, 2333 (1997).
[16] J. I. Steinfeld, *Molecules and Radiation: An Introduction to Modern Molecular Spectroscopy* (Harper & Row, New York, 1974).
[17] T. Helgaker *et al.*, *DALTON a molecular electronic structure program—release 1.2*, 2001, see http://www.kjemi.uio.no/software/dalton/dalton.html.
[18] F. F. Guimarães, F. Gel'mukhanov, A. Cesar, and H. Ågren, Chem. Phys. Lett. **405**, 398 (2005).
[19] B. Zhao and S. Zhu, Opt. Eng. **38**, 2129 (1999).
[20] J. Ohkubo, T. Kato, H. Kono, and Y. Fujimura, J. Chem. Phys. **120**, 9123 (2004).
[21] TOPAS Model 4/800 (Femtosecond version) wavelength range from 1150 to 2600 nm, see http://www.lightcon.com/lc/scientific/scientific.htm.
[22] A. Yagishita, E. Shigemasa, and N. Kosugi, Phys. Rev. Lett. **72**, 3961 (1994).
[23] R. Guillemin, E. Shigemasa, K. Le Guen, D. Ceolin, C. Miron, N. Leclercq, K. Ueda, P. Morin, and M. Simon, Rev. Sci. Instrum. **71**, 4387 (2000).
[24] K. Ueda, J. Phys. B **36**, R1 (2003).
[25] S. Chelkowski, P. B. Corkum, and A. D. Bandrauk, Phys. Rev. Lett. **82**, 3416 (1999).
[26] D. Sugny, A. Keller, O. Atabek, D. Daems, C. M. Dion, S. Guerin, and H. R. Jauslin, Phys. Rev. A **69**, 033402 (2004).